ORNL/TM-2023/2852

Characterizing PuO_2 Powder at Oak Ridge National Laboratory for the Multi-Lab Plutonium Process Signatures Campaign FY 2022

Luke R. Sadergaski
Hunter B. Andrews
Andrew J. Miskowiec
David G. Abrecht
Sam K. Schrell

February 2023

OAK RIDGE National Laboratory

ORNL IS MANAGED BY UT-BATTELLE LLC FOR THE US DEPARTMENT OF ENERGY

DOCUMENT AVAILABILITY

Reports produced after January 1, 1996, are generally available free via OSTI.GOV.

Website www.osti.gov

Reports produced before January 1, 1996, may be purchased by members of the public from the following source:

National Technical Information Service
5285 Port Royal Road
Springfield, VA 22161
Telephone 703-605-6000 (1-800-553-6847)
TDD 703-487-4639
Fax 703-605-6900
E-mail info@ntis.gov
Website http://classic.ntis.gov/

Reports are available to US Department of Energy (DOE) employees, DOE contractors, Energy Technology Data Exchange representatives, and International Nuclear Information System representatives from the following source:

Office of Scientific and Technical Information
PO Box 62
Oak Ridge, TN 37831
Telephone 865-576-8401
Fax 865-576-5728
E-mail reports@osti.gov
Website https://www.osti.gov/

ORNL/TM-2023/2852

Radioisotope Science and Technology Division

CHARACTERIZING PuO_2 POWDER AT OAK RIDGE NATIONAL LABORATORY FOR THE MULTI-LAB PLUTONIUM PROCESS SIGNATURES CAMPAIGN FY 2022

Luke R. Sadergaski
Hunter B. Andrews
Andrew J. Miskowiec
David G. Abrecht
Sam K. Schrell

February 2023

Prepared by
OAK RIDGE NATIONAL LABORATORY
Oak Ridge, TN 37831-6283
managed by
UT-BATTELLE, LLC
for the
US DEPARTMENT OF ENERGY
under contract DE-AC05-00OR22725

CONTENTS

LIST OF FIGURES

ABBREVIATIONS

DRA	diffuse reflectance accessory
DRS	diffuse reflectance spectroscopy
LIBS	laser-induced breakdown spectroscopy
FWHM	full width at half maximum
ORNL	Oak Ridge National Laboratory
PC	principal component
PCA	principal component analysis
pXRD	powder X-ray diffraction
RCT	radiological control technician
SEM	scanning electron microscopy
UV-Vis-NIR	ultraviolet–visible–near infrared

ACKNOWLEDGMENTS

Funding for this project was provided by the National Nuclear Security Administration (NA-22). This work was supported by the Multi-Lab Plutonium Process Signatures Project.

ABSTRACT

This report highlights the development of advanced analytical capabilities at Oak Ridge National Laboratory to characterize PuO_2 powder to support the Multi-Lab Plutonium Process Signatures Campaign in FY 2022. Two samples from a batch of 76 statistical precipitation runs were packaged and shipped from Pacific Northwest National Laboratory to Oak Ridge National Laboratory at the beginning of FY 2022. Techniques were used to characterize the sample, including powder X-ray diffraction, Raman spectroscopy, and diffuse reflectance spectroscopy. A brief description of each technique, the results and discussion, and future work are described in this report. Opportunities to expand current capabilities and include additional analytical capabilities for the next campaign will also be discussed.

1. BACKGROUND

1.1 INTRODUCTION

Determining process history, age, and storage conditions of interdicted nuclear materials is key to the nuclear forensics and nuclear nonproliferation fields. This determination necessitates a comprehensive understanding of the physical and chemical properties of nuclear materials. Often, state-of-the-art analytical capabilities are required to characterize materials. Although Pu has been produced and processed for numerous decades,[1] many fundamental structural and chemical properties of key processing species are not fully understood. Working with Pu is challenging because of safety and regulation, radiotoxicity, chemical complexity, and weaponization stigmas. Thus, many Pu compounds are understudied and require a focused effort, such as the Multi-Lab Plutonium Process Signatures effort, to fully characterize such materials.

Few studies have used optical spectroscopy to characterize the Pu compounds involved in industrial-scale fuel and waste reprocessing plants, where Pu dioxide is routinely produced in large quantities. Most studies have focused on Raman spectroscopy, which is a vibrational technique, to characterize PuO_2 samples.[2] More recently, diffuse reflectance infrared Fourier transform spectroscopy, in conjunction with Raman spectroscopy, was used to monitor the decomposition of Pu(IV) oxalate to PuO_2 at various temperatures.[2] Another complementary technique, diffuse reflectance spectroscopy (DRS), can provide detailed information about metal–ligand electronic interactions. The data can be acquired quickly in the short-wave infrared region (900–1,600 nm) compared with other techniques such as diffuse reflectance infrared Fourier transform spectroscopy. A recent paper demonstrated that DRS and principal component analysis (PCA) can be used to determine the production history of PuO_2.[3]

Oak Ridge National Laboratory (ORNL) also has unique analytical capabilities for studying PuO_2 and potentially synthesizing PuO_2 at relatively large scales in the future, if desired. The ability to reproduce signatures that describe material properties, and the characterization results and interpretation must be validated and verified. Collaborations with multiple national laboratories can help account for variables that could affect how the specimens are characterized with different instruments and parameters. Unique capabilities at ORNL could also be leveraged to monitor aqueous Pu processing streams.[4]

It would also be useful to explore variables that may account for product material characteristics, such as subtle differences in process execution and performance based on operator technique, equipment, and climate. The expertise and capabilities currently held at ORNL can be leveraged to reproduce specific unit operation conditions of interest. The Radiochemical Engineering Development Center at ORNL, where the ^{238}Pu production program has been established in recent years, is a Hazard Category II nuclear facility with hot cells and glove box laboratories used for chemical separations and oxide production operations. ORNL also has the material characterization capabilities necessary for studying PuO_2 products, including

X-ray diffraction, Brunauer–Emmett–Teller surface area, particle size analysis, inductively coupled plasma–mass spectrometry, ultraviolet–visible–near infrared (UV-Vis-NIR) and Raman spectroscopy, scanning electron microscopy (SEM), laser-induced breakdown spectroscopy (LIBS), and others.

1.2 PRIMARY GOALS

The Multi-Lab Plutonium Process Signatures project is working toward the discovery of forensic signatures in PuO_2 precipitation processes and determining persistence in PuO_2 product. Previous efforts developed a set of 76 PuO_2 runs in which conditions were selected using experimental design. Data have already been collected on the resulting materials with techniques, including X-ray diffraction, infrared spectroscopy, color analysis, trace chemical analysis, and SEM. Statistical modeling of the various data sources is in progress but is outside the scope presented in this report. Researchers plan to collect overlapping data sets (e.g., powder X-ray diffraction [pXRD] and Raman spectroscopy) and unique data sets (e.g., DRS) to help validate current technologies and expand capabilities. The primary goal in FY 2022 was to establish a workflow for analyzing PuO_2 samples and to provide data needed to identify robust signatures indicative of different processing methods.

Two PuO_2 samples (R22 and R67) from the statistical precipitation runs were shipped from Pacific Northwest National Laboratory and arrived at ORNL early in FY 2022. Each sample comprised triplicates, 50 mg each, for a total of 300 mg PuO_2. The overarching goal of this work was to establish administrative and technical capabilities to characterize PuO_2 samples. Traditionally speaking, ORNL is not a Pu lab, so research related to Pu can be challenging for many logistical reasons unrelated to the science. More specifically, the core analytical techniques tested in this work include pXRD, Raman spectroscopy, and DRS. Additional techniques (e.g., LIBS) were also considered and could be included in future work (see Section 6.1). This report elaborates on the progress made in FY 2022 and the most opportune next steps.

2. POWDER X-RAY DIFFRACTION

2.1 MOTIVATION

The pXRD characterization technique is commonly used for phase identification, sample purity, dimensions, and the morphology of crystalline material. The technique consists of an X-ray source, a sample stage, a detector, and a method to vary the incident angle. X-rays diffract (i.e., scatter) when interacting with atoms in a crystal and are collected as a diffraction pattern. The analysis is complementary with various microscopic and spectroscopic methods. This bulk technique can be correlated with microscopy data to determine whether microscopic observations on a small number of particles are representative of the overall material.

2.2 RESULTS AND DISCUSSION

Patterns from pXRD were acquired with a Rigaku Miniflex II in a negative-pressure glove box. The Miniflex system is equipped with a six-sample changer and a monochromatic Cu Kα (1.5406 Å) X-ray source. Patterns were collected from 15°–80° 2θ using a step size of 0.02 and a scan rate of 0.35°/min. The voltage and current of the X-ray tube were 30 kV and 15 mA, respectively. Powders (~7 mg) were placed in a 2 mm width × 1 mm deep plate and gently pressed in place. The samples were not sealed; therefore, each peak corresponds to a PuO_2 nuclear Bragg peak location. The pXRD analysis took several hours per pattern.

Characteristic cubic powder patterns for each PuO_2 sample were collected. No secondary phases were identified. Phases analysis was confirmed by comparison to the International Centre for Diffraction Data

database. The average pattern of triplicates for each sample is shown in Figure 2-1. On average, sample R22 had a lower intensity and broader peaks than R67. However, the patterns are similar.

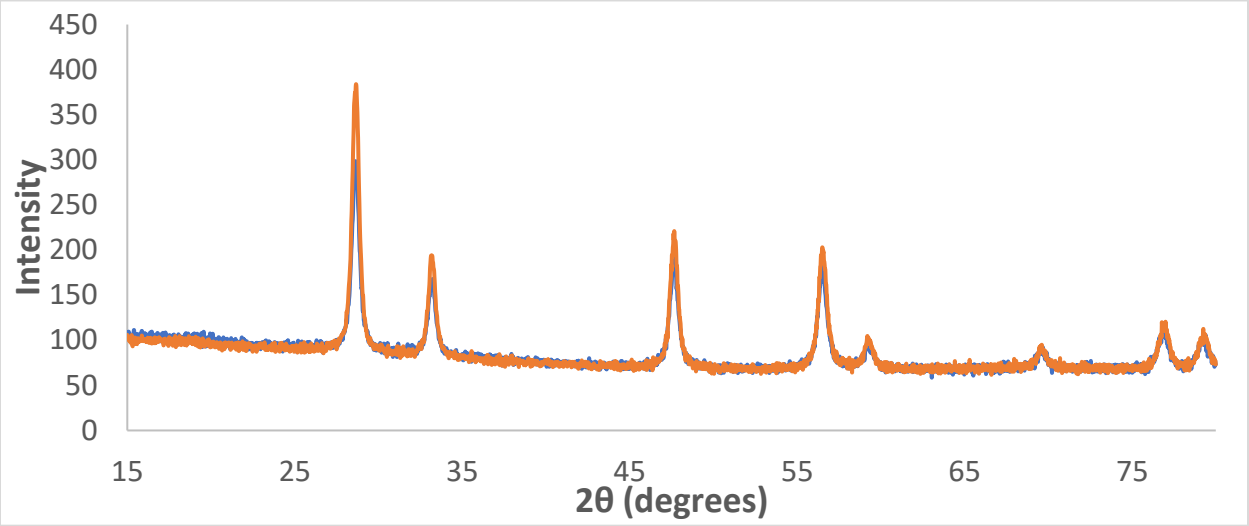

Figure 2-1. Average pXRD pattern for each sample (blue) R22 and (orange) R67.

2.3 NEXT STEPS

Diffraction patterns can be used to refine the parameters of a crystal structure by Rietveld refinement. Future work will consist of performing a full-pattern Rietveld refinement on the data to determine unit cell parameters. This refinement can also define properties such as crystallite size and the strain parameter. This refinement will be performed using conditions consistent with other researchers in the project and compared with data acquired at Pacific Northwest National Laboratory and Los Alamos National Laboratory. These labs used a sample containment vessel which introduced baseline artifacts whereas the data presented in this report were collected without any containment.

3. RAMAN SPECTROSCOPY

3.1 MOTIVATION

Raman spectroscopy has been used ubiquitously in the literature as a tool to investigate α decay damage and age since calcination.[5–9] The technique can also be used to detect PuO_2 in different host matrices (e.g., glass) and to investigate the crystalline order and morphology of PuO_2 grains and aggregates. These characteristics are sensitive to the initial production conditions. Quantification of various properties related to production history is possible by measuring the ratio of Stokes and anti-Stokes band intensities, band position, and the full width at half maximum (FWHM) of various peaks in the spectrum. ORNL has glove box and benchtop Raman instrumentation amenable to characterizing PuO_2. Researchers for this work had success characterizing the PuO_2 samples with the cold benchtop instrument.

The most intense PuO_2 band in the Raman spectrum, the T_{2g} band, was observed near 477 cm^{-1}. This band is asymmetric because of phonon confinement. This band shifts to higher energies for samples calcined at higher temperatures. It also becomes more symmetric with increasing calcination temperature, suggesting that the crystallite size increases. The FWHM of the T_{2g} band is related to the strain and disorder in the material. This parameter is related to the calcination temperature, and the other PuO_2 bands are related to the precursor compound (e.g., oxalate).

The Γ1 to Γ5 and Γ1 to Γ3 electronic transitions tend to shift to higher wavenumbers with increasing calcination temperatures, which is indicative of increased ordering in the crystal structure. These transitions were identified near 2,136 cm^{-1} for Γ1 to Γ5 and 2,640 cm^{-1} for Γ1 to Γ3 for each sample.[9] The very weak 1LO2 band, commonly referred to as the *defect band*, is composed of two Lorentzian bands at lower calcination temperatures (350°C–750°C) and a single Lorentzian band near 578 cm^{-1} for higher temperatures. The ingrowth of these bands provides a useful indicator for the calcination age.

3.2 RESULTS AND DISCUSSION

3.2.1 Raman spectra

Raman spectra were collected using a Renishaw inVia Raman microscope with a 50× objective (Figure 3-1) and a 532 nm laser operating at 1% or 5% power. A quick scan acquires data from -25 to 1,250 cm^{-1}, and the acquisition time is several minutes. Spectra were collected above and slightly below the Rayleigh scatter line (0 cm^{-1}) to allow a wavelength calibration using the 532 nm laser. The extended scan goes beyond 3,300 cm^{-1} and takes approximately 30–60 minutes to acquire a useful spectrum. Integration times can be adjusted to achieve the desired ratio level of signal-to-noise.

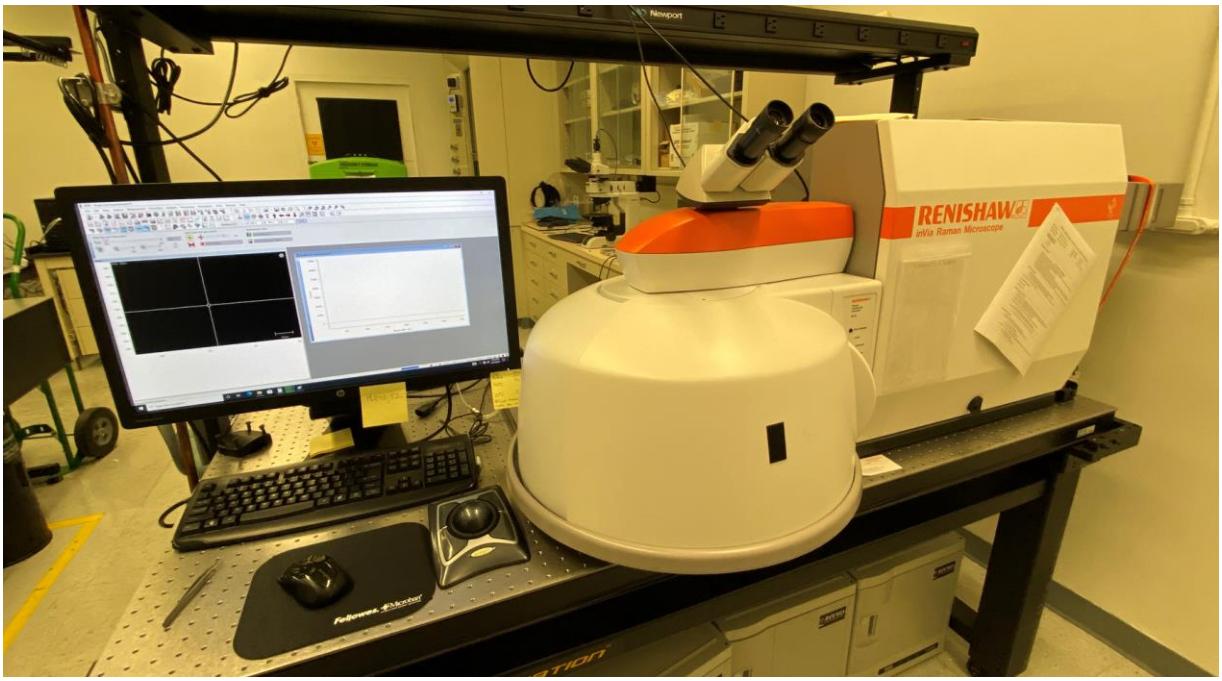

Figure 3-1. Renishaw inVia Raman microscope.

Researchers in this work initially attempted to use a Horiba iHR320 imaging spectrometer equipped with a MicOS microscope. Although excellent spectra could be measured using a surrogate (CeO_2, white powder), no signal was detected from PuO_2 or UO_2 (black powders). The reflection optics likely were not sensitive enough. Based on experience thus far, a high-end Raman microscope is essential when measuring Raman spectra of weakly scattering and dark-colored actinide oxide materials.

Samples were prepared by sealing approximately 1 mg of PuO_2 between two quartz slides (Figure 3-2). The bottom slide had a recess. Future work will use off-the-shelf slides with a concave depression cavity. The samples were prepared in a negative-pressure glove box and overpacked into a radiological fume hood. A radiological control technician (RCT) surveyed the slides, which were decontaminated if necessary. Then, the edges were glued, and finally, tape was applied to the edges as a secondary

containment layer. After approval from RCTs, the samples were ready for analysis on the cold instrument. This preparation technique works very well. However, the samples appeared to have a shelf life. Over time (~6-12 months), the quartz window seemed to degrade, and we observed more noise in the Raman spectra. This will be evaluated in greater detail in the next campaign.

Figure 3-2. Sample of approximately 1 mg PuO_2 powder in quartz slide.

Optical images of PuO_2 particles were acquired with most Raman spectra (Figure 3-3). The particles were typically between approximately 10 and 100 μm in diameter. The disparate colors were likely an artifact of the incident light and not indicative of unique sample types. The authors assume this explanation because Raman spectra were consistent when collected at various points throughout each particle.

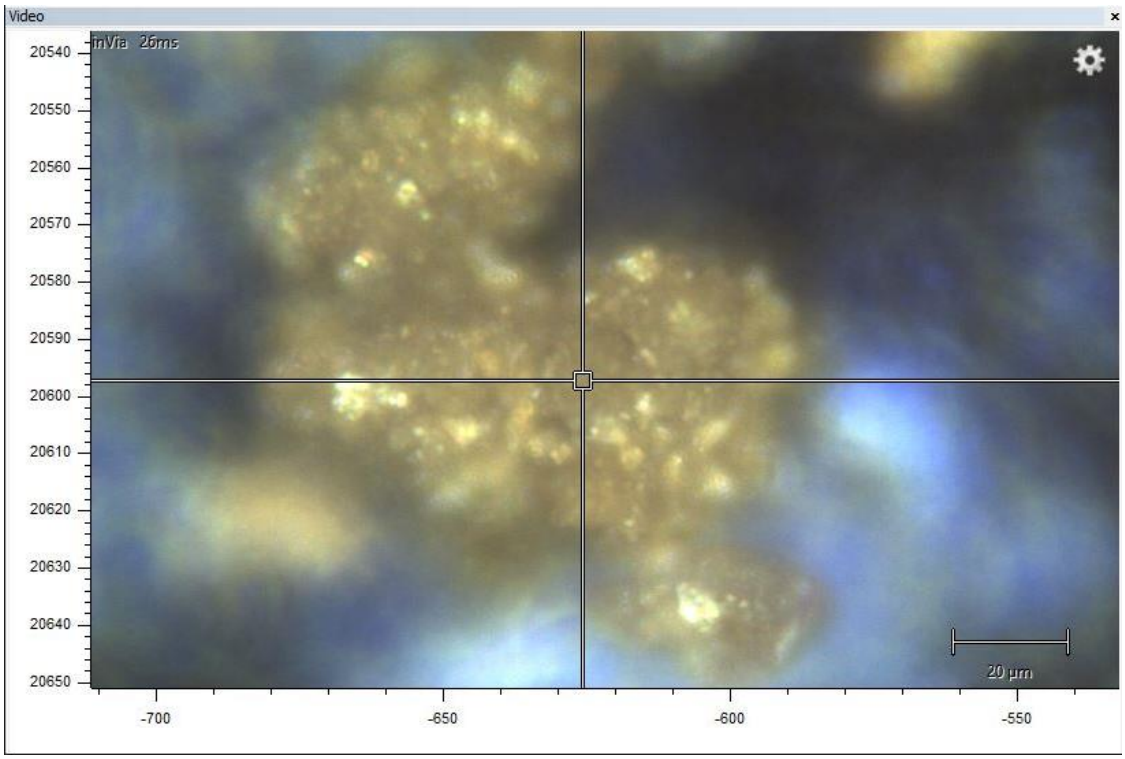

Figure 3-3. Optical image of a PuO_2 particle using the Raman microscope with 50× objective.

The Raman spectrum for sample R67s3 is shown in Figure 3-4. The Raman spectrum of PuO_2 is complex, particularly as it ages.[8] The dominant bands were identified and assigned as 479 cm^{-1} for the T_{2g}, 581 cm^{-1} for 1LO2 (disorder), 1,163 cm^{-1} for 1LO2 (overtone), 2,135 cm^{-1} for an electronic band, and 2,635 cm^{-1} for another electronic band. The FWHM for the T_{2g} was 15.3 ± 0.5 cm^{-1}. The asymmetry of the 1LO2 defect band comprised two Lorentzian peaks, which is commonly indicative of a lower calcination temperature (350°C–750°C). Several additional peaks were also identified near 655, 1,056, 2,258, 2,950, and 2,998 cm^{-1}. These bands are indicative of samples prepared from different Pu-bearing precursors such as oxalate, fluoride, or nitrate. These bands are consistent with a previous study, suggesting that they are related to oxalate impurities.[2]

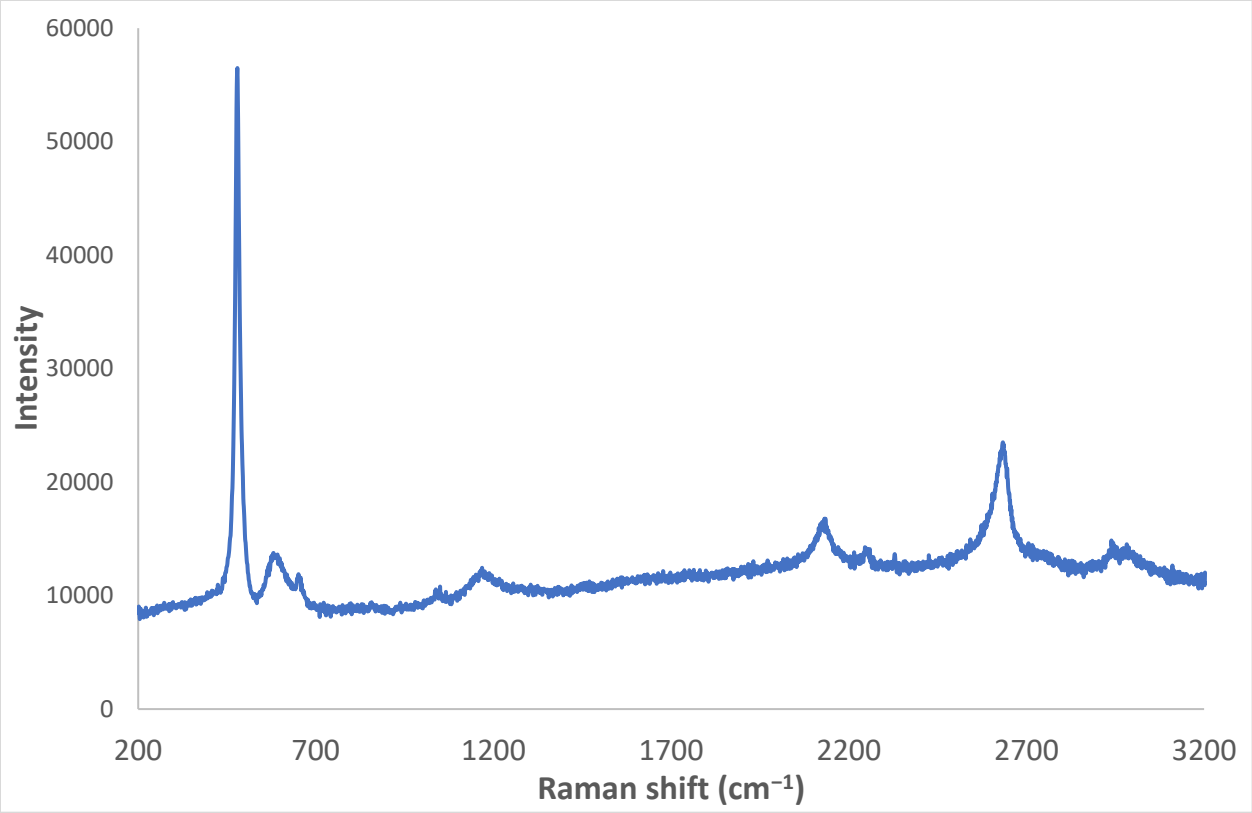

Figure 3-4. Raman spectrum for sample R67s3 collected on September 27, 2022.

The Raman spectrum for sample R22s3 is shown in Figure 3-5. The dominant bands were identified and assigned as 477.5 cm^{-1} for the T_{2g}, 581 cm^{-1} for 1LO2 (disorder), 1,163 cm^{-1} for 1LO2 (overtone), 2,135 cm^{-1} for an electronic band, and 2,635 cm^{-1} for another electronic band. The FWHM for the T_{2g} was 18.4 ± 0.5 cm^{-1}. The asymmetry of the 1LO2 defect band appears to be composed of two Lorentzian peaks, which is commonly indicative of a lower calcination temperature (350°C–750°C). The other bands characterized in sample R67 were identified in R22 but are not as obvious. This subtlety suggests that fewer (if any) oxalate impurities are present in this sample.

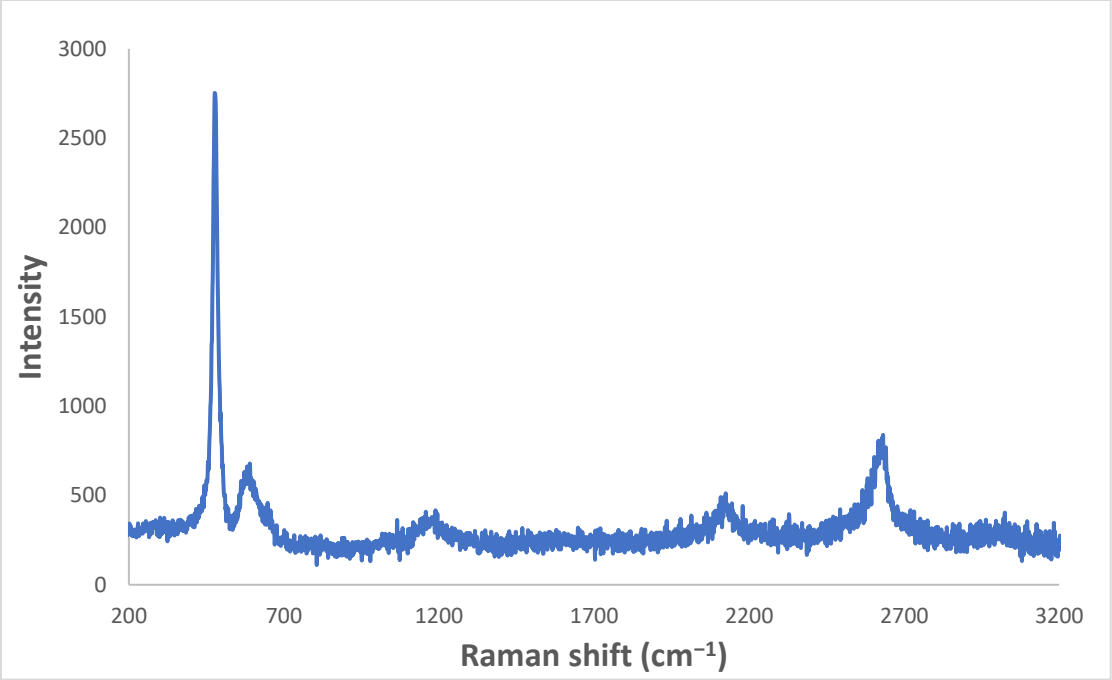

Figure 3-5. Raman spectrum for sample R22s2.

Raman spectra were generally reproducible between samples. An example spectrum is shown in Figure 3-6. This figure compares samples R22s2 and R22s3, which were prepared and analyzed separately. Each measurement used a 50× objective, laser power (5%), and a 10 s integration time. The analysis time was approximately 3 min/sample. The peak at 0 cm^{-1} is the laser line.

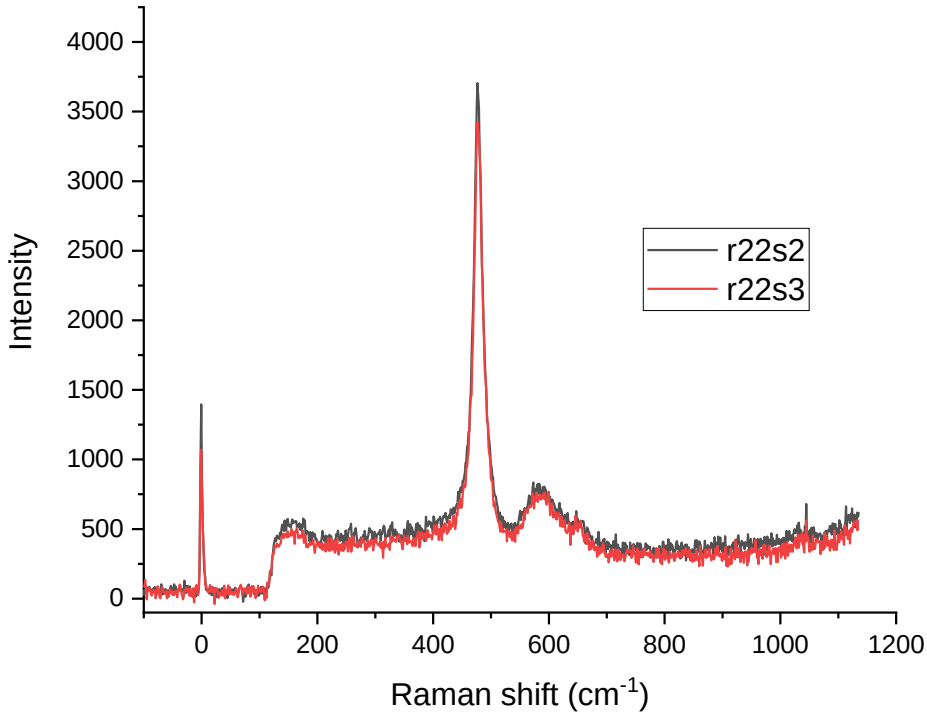

Figure 3-6. Raman spectrum for samples R22s2 and R22s3.

3.2.2 2D Raman maps and PCA

PCA is a power exploratory data analysis tool used primarily to find patterns in large data sets. It is a bilinear modeling method, also known as a *projection method*, that projects information from the original variables onto a subset of latent variables (i.e., principal components [PCs]). PCs explain some portion of the information from the original data set, and subsequent PCs contain less information than the previous one. PCA is an essential multivariate data analysis technique used to quantify the amount of useful information in data sets and detect outliers. This work applied PCA to Raman spectral data sets to determine the reproducibility of the spectral features. Researchers used the Unscrambler X software version 10.4 and a NIPALS algorithm for PCA. The Hoteling's T^2 statistic helped to identify outliers or situations where the process was not operating within normal conditions. Leverages were also useful for detecting a sample far from the center of the multivariate space described by the model. PCA leverages indicate how much variables influence the PCA model. Samples with high leverage differed from the average samples and highly influenced the model. If these high-leverage samples were outliers, then it was best to remove them.

This work also completed additional Raman tests on sample R22. One test included an analysis of 10 separate particles, with three regions of one particle (12 total spectra). The second test included a map with 100 scans at 2 × 2 μm increments (total area of 20 × 20 μm). Spectral data were analyzed by PCA. Applying baseline offset corrections and scatter correction, such as standard normal variate analysis, did not improve the analysis. Spectra were simply mean-centered prior to PCA and chopped from approximately 330–720 cm^{-1}. PCA calibration statistics were compared with a full cross validation.

Slight differences in the focus (i.e., Z-height) cause focal point and collection optic differences which change the peak intensity and background between Raman measurements. If the only difference between measurements is focus distance, then parameters like FWHM should be constant. Differences in spectrum characteristics (e.g., FWHM) may indicate differences between particles or spots within a given particle.

Separate particles. The region from 300 to 720 cm^{-1} was analyzed. The first PC (PC-1) described 99.26% of the explained variance in the analysis of 10 separate particles, and PC-2 described 0.61%. Only one spectrum (i.e., particle) had a significant score related to PC-2, so it could be considered an outlier (particle 5). The cross validation–explained variance did not increase substantially beyond two PCs.

When only the T_{2g} band (430–530 cm^{-1}) was modeled by PCA, PC-2 became more important. In a 2D scores plot comparing PC-1 and PC-2, each sample fit within a Hotelling's T^2 Ellipse with a critical limit (i.e., *p*-value of 25%). This limit indicates that all samples were described by the model. However, when this value was adjusted to a *p*-value of 25%, then two samples fell outside of the ellipse (see Figure 3-7). In this PCA model, PC-1 described 98.74% of the explained variance, and PC-2 described an additional 1.14%. This second component appeared to be significant when the scores and loadings for each sample were examined (Figure 3-8).

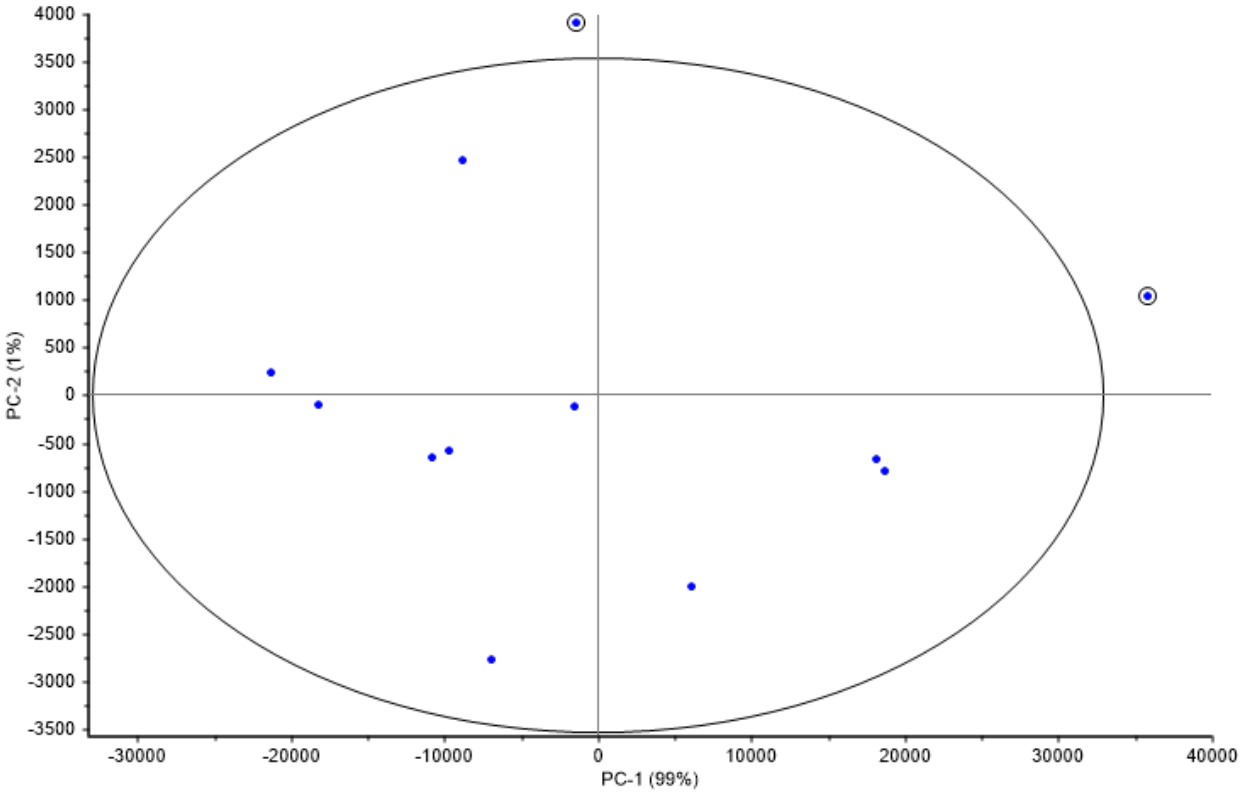

Figure 3-7. Two dimensional scores plot of PC-2 vs. PC-1 for the 12 Raman spectra.

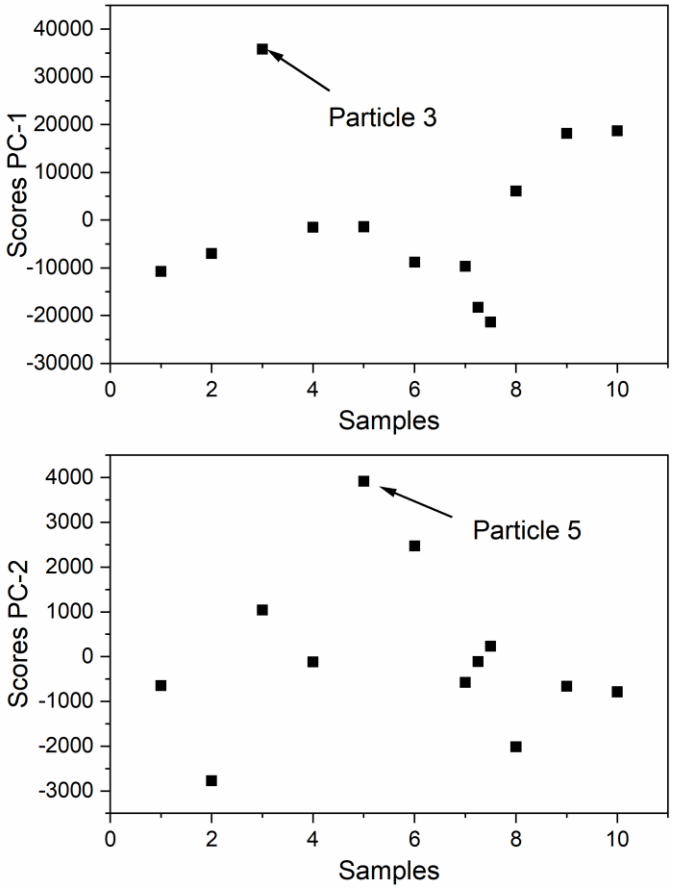

Figure 3-8. PCA scores for each sample (a) PC-1 and (b) PC-2 with outliers noted.

Voigt peak fitting for each spectrum revealed that the FWHM of particle 3 was 19.6 ± 0.4 cm^{-1} and 18.5 ± 0.5 cm^{-1} for particle 5. These values are statistically different at 1 σ. This difference suggests that the instrument acquisition was inconsistent between particles, the quartz window was compromised, or differences may exist between sample particles. Although these values are similar, the quantification of various PuO_2 properties relies on the FWHM of the T_{2g} band. This value should be explored in more detail in future work. Raman spectra for particles 3 and 5 are shown in Figure 3-9.

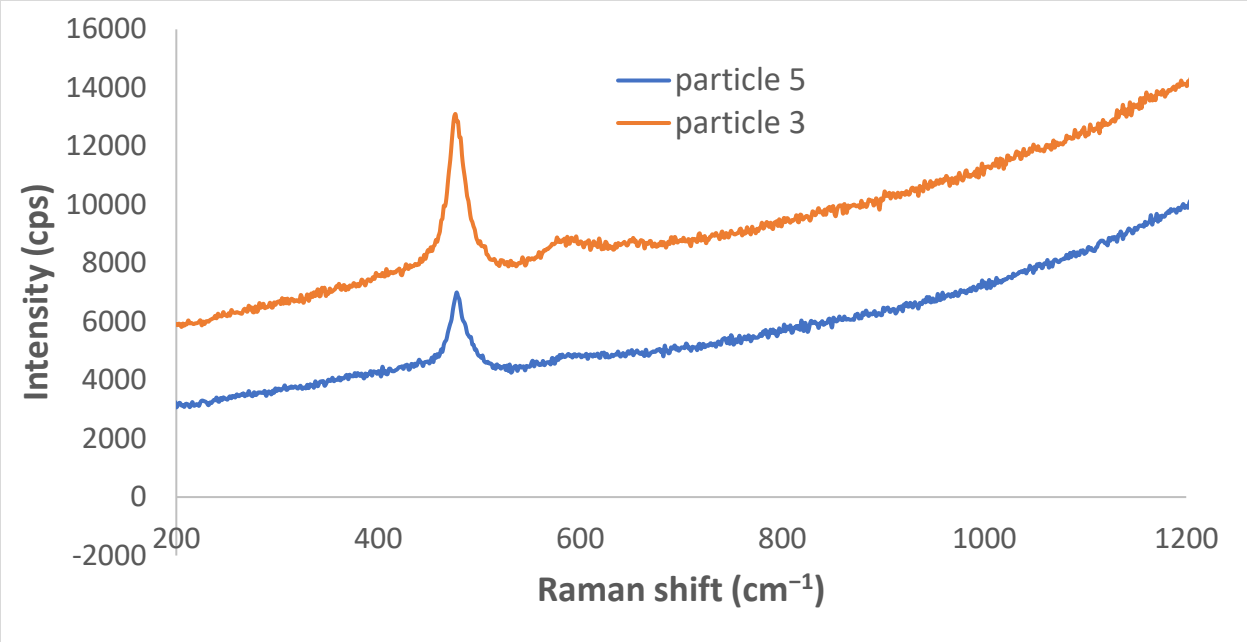

Figure 3-9. Raman spectra for particles 3 and 5.

Raman map. The area analyzed by the Raman map and the corresponding spectra are shown in Figures 3-10 and 3-11, respectively. PCA analysis was used to measure sample/instrument consistency throughout a large portion of the PuO_2 particle. PC-1 described 99.49% of the explained variance in the map, and PC-2 described 0.42%. More than 99% of the structured variation in the data sets were described by one component (i.e., spectral feature), and the feature was consistent between samples. This consistency does not mean that the second component is not also significant. When only the T_{2g} band was analyzed, PC-1 and PC-2 described 98.87% and 1.03% of the explained *X*-variance, respectively. Again, PC-2 became more significant when less of the Raman spectrum was analyzed, and only the most relevant features (i.e., T_{2g}) band were modeled.

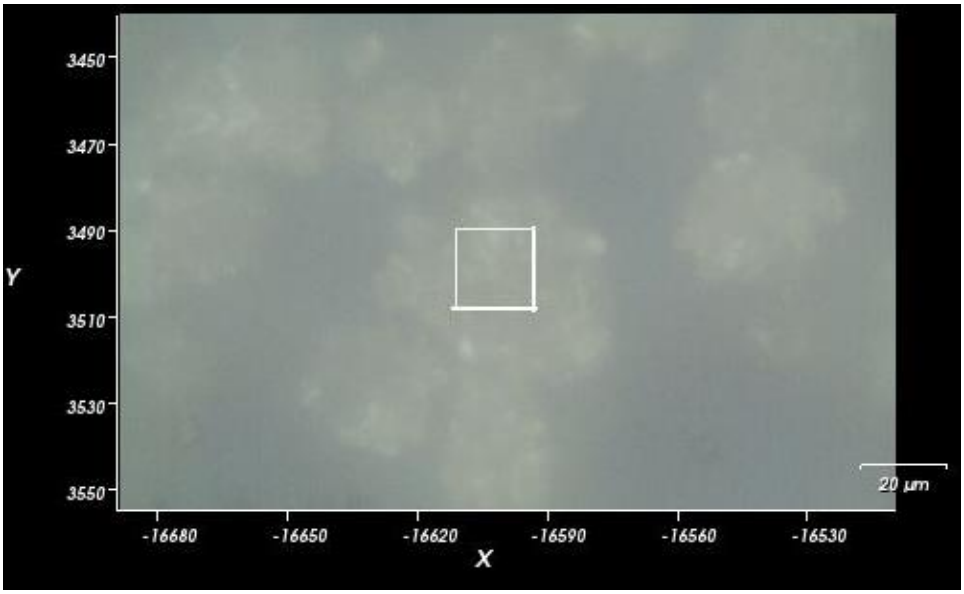

Figure 3-10. Area analyzed by the Raman map.

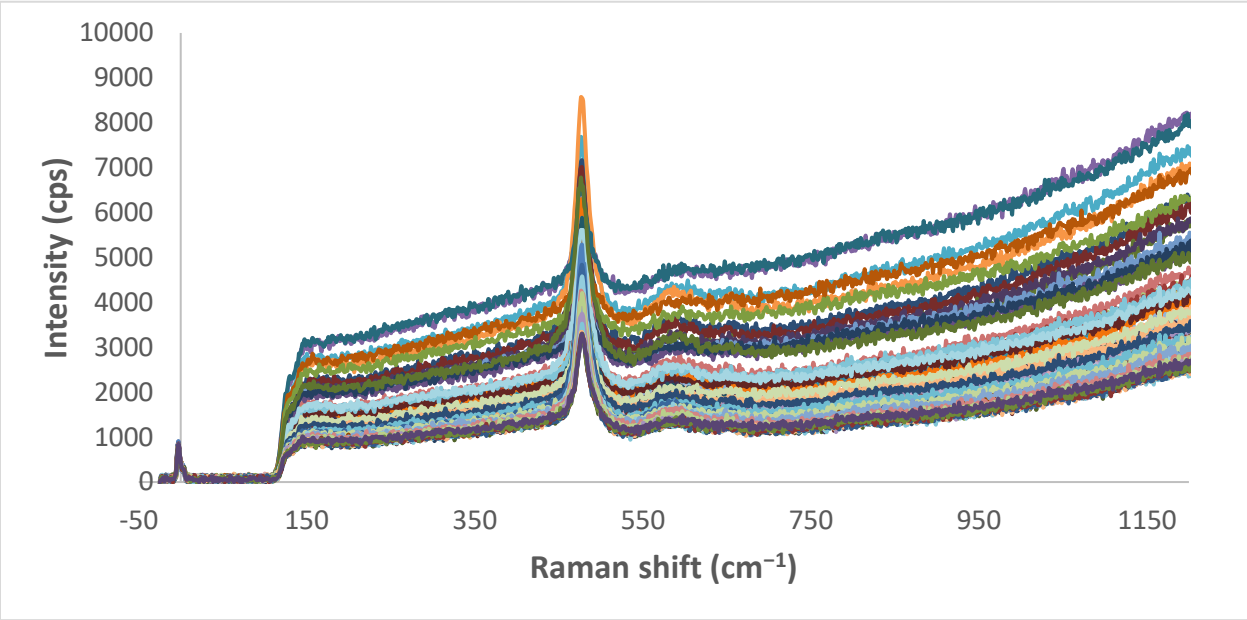

Figure 3-11. Raman spectra collected during map of sample R22s3 (raw data).

In a 2D scores plot (Figure 3-2) comparing PC-1 and PC-2, most spectra fit within a Hotelling's T^2 Ellipse with a critical limit (i.e., *p*-value of 10%). The leverage values for these samples also fall outside of the critical *p*-value (10%). Thus, these spectra are likely not representative of the sample.

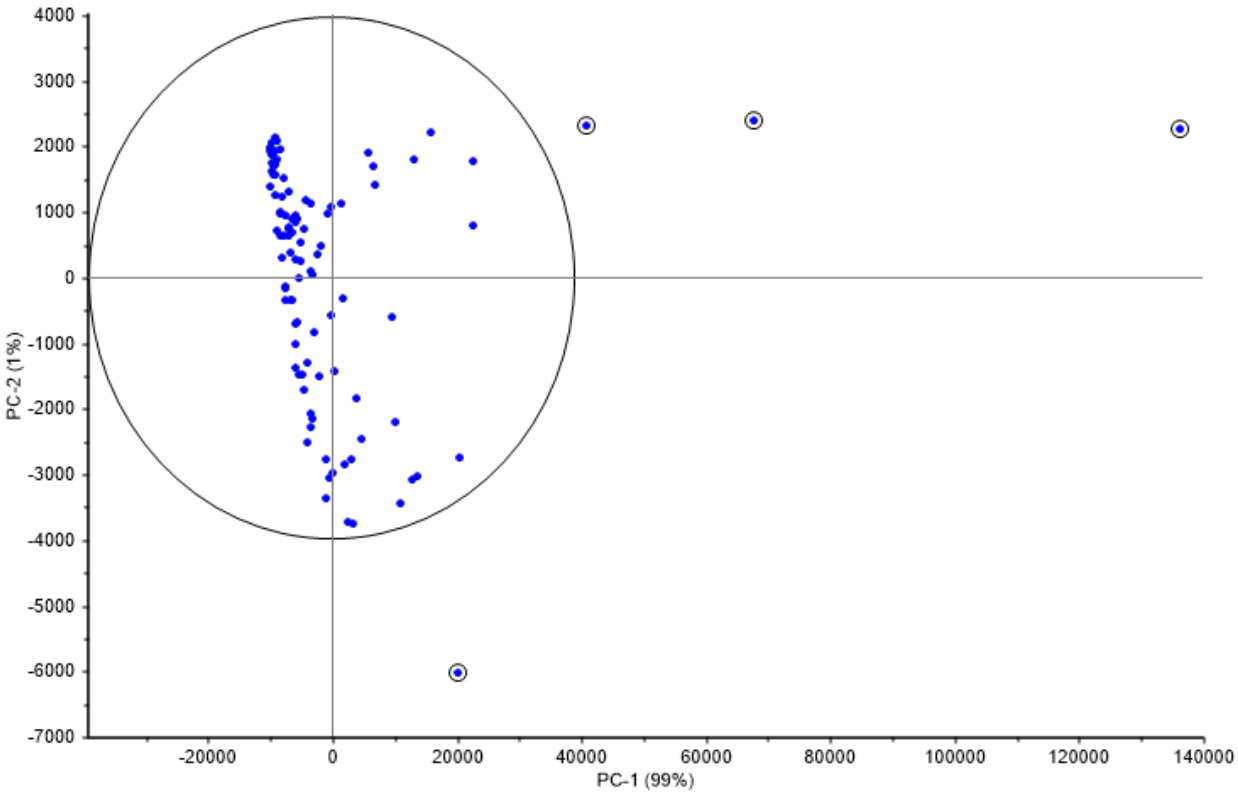

Figure 3-12. 2D scores plot of PC-2 vs. PC-1. Outliers are marked.

An outlier spectrum (R2) identified in Figure 3-2 was compared with a nonoutlier spectrum (R4), and FWHM values were 17.7 and 18.7 cm^{-1}, respectively. In general, the outliers in Figure 3-2 had narrower FWHM and a higher baseline offset.

This work suggests that collecting numerous Raman spectra of multiple particles is important before reporting defining properties such as FWHM. A more exact number cannot be reported at this time because of a limited data set. This PCA and Raman analysis primarily focused on the T_{2g} band of one sample. Future measurements could focus on additional bands in the spectrum of PuO_2 and determine whether components with <1% explained variance are significant.

Applying preprocessing transformations such as standard normal variate analysis resulted in PCA models that described <80% of the structured variation in the data set. Standard normal variate analysis is a row-oriented transformation that removes multiplicative scatter interferences and particle size effects by centering and scaling each spectrum. Although preprocessing transformations are expected to improve the analysis, the opposite effect was generally observed.

3.3 NEXT STEPS

The authors intend to analyze the next set of samples in Campaign 2 (FY 2023) over time to help gather information related to the rate of accumulated defect structure from α decay. Researchers also intend to help identify robust signatures and sample acquisition parameters amenable to real-world samples. Most Raman spectroscopy studies analyze single particles over time without moving the particles or changing instrument parameters to remove any variation that is not related to the sample chemistry. Future work will perform a systematic study to better understand how sample size and instrument settings affect measurement behavior and data interpretation. Applying Raman in forensic applications would benefit

from this kind of study. This method should be addressed to understand if single samples represent the bulk process and how to capture statistically significant data with minimal analytical effort.

Parameters may be selected for this study using experimental design. Design of experiments, which is a statistical approach to select samples/variables, can be used for planning experiments and data analytics. Design of experiments is useful for minimizing the number of samples required in the data set while accounting for the structured variation of the factor space.

4. DIFFUSE REFLECTANCE SPECTROSCOPY

4.1 MOTIVATION

A wide range of the colors of PuO_2 have been observed, and these colors are poorly understood.[10] Although various colors of PuO_2 are well-known, the cause of the color change is not. ORNL could rigorously measure the color of the oxide material using UV-Vis-NIR diffuse reflection (i.e., absorption) spectroscopy using an integrating sphere in a glove box. This technique is sensitive to Pu valences. ORNL's new Cary-6000i instrument with the diffuse reflectance accessory (DRA) can be used for these measurements.

This work proposed to improve the ability to use quantitative color analyses as an indicator of process provenance for nuclear forensics assessments through a combined computational and experimental evaluation of the origins of color differences in PuO_2. Color differences in calcined PuO_2 have long been noted in their production, with descriptions of the color including yellow,[11] olive-green,[12,13] olive-brown,[12] amber,[14] black,[14,15] dark khaki,[16] and yellow-green[11]. These differences in color have been attributed to various process differences, including calcination temperature,[17] initial Pu compound,[1] stoichiometry,[5] and microstructure,[4] but the significance of each of these effects on the apparent or spectral color has not been fully explored. Improving understanding of these effects will lead to an improved ability to use color for provenance determinations.

Traditionally, color is characterized by matching the sample color to a color swatch found in Munsell charts. Although this method has proven to be a valuable means of assigning color to samples, it is generally considered to be a qualitative test; color assignment using this method is subjective and can vary depending on the incident lighting, the operator's color vision and perception of color (including optical mixing effects and other optical illusions), and other environmental factors.[18] Additionally, Pu compounds commonly exhibit dichroism, pleochroism, and the alexandrite effect,[19–22] which can all have significant effects on the perceived color. Alternatively, techniques exist for collecting electromagnetic spectra for samples in the UV-Vis-NIR region, allowing for the quantitative determination of how photons interact with the samples to produce color. One such technique, UV-Vis-NIR DRS, collects reflected electromagnetic intensities in the region of 300–1,700 nm that correspond to electronic and/or vibrational energy levels in the sample for the quantitative evaluation of sample color. This measurement method is also able to determine if environmental artifacts are present, such as absorption bands corresponding to water or impurities such as quartz from the sample holder or other host matrices.[23,24]

This work evaluated DRS for the collection of UV-Vis-NIR absorption spectra from PuO_2 to differentiate the effects of physical or process-derived effects on the quantitative color. Unique spectral characteristics were identified to help provide a more complete picture of the sample history and how it relates to other characteristics previously studied.

4.2 RESULTS AND DISCUSSION

Spectrophotometry, or absorption spectroscopy, is used to quantitatively measure the amount of light absorbed by a molecule as a function of wavelength in many lab- and industrial-scale applications. Measurements were performed on a Cary-6000i instrument using a DRA, which is also known as an *integrating sphere*. The DRA can be used for reflectance, transmission, or absorption measurements of opaque, turbid, and/or reflective substances. This work used a reduced slit to focus the measurements on the sample. Future work could benefit from using a small spot kit to reduce the amount of sample needed.

Samples were prepared by 'sandwiching' ~ 20 mg of PuO_2 between quartz slides (Figure 4-1). Each sample was prepared by this method. However, we lost several samples due to radiological contamination. These were sent back to the glove box and may be analyzed in the future. The DRS spectra for two samples is shown in Figure 4-2. The spectra were relatively consistent, and several bands are comparable to observations documented in the literature.[3]

Figure 4-1. PuO_2 sample prepared on a quartz slide sandwich.

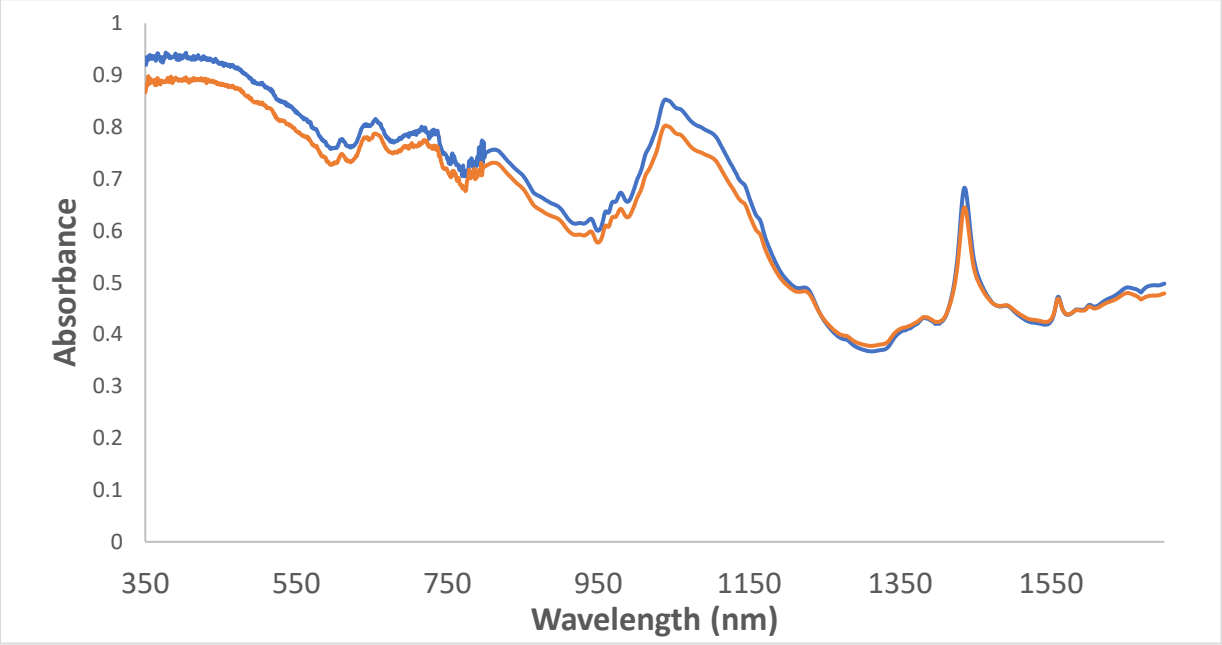

Figure 4-2. Diffuse reflectance spectra of PuO_2 samples (blue) R67S2 and (orange) R67S3.

4.3 NEXT STEPS

With complicated spectra, such as that expected from PuO_2, modeling the electromagnetic interactions in the solid can help to interpret the experimental results. DRS modeling efforts have been applied to the technique over a wide range of assumptions and accuracies, from very simplified continuum models of material interfaces to statistical evaluations of particle interactions and modern computational techniques examining individual photons, including Monte Carlo and ray-tracing techniques.[25,26] Regardless of the technique chosen, these modeling methods generally require a complex refractive index for the material. For PuO_2, these values were recently reported for epitaxial thin films grown on yttria-stabilized zirconia,[27] enabling the modeling of diffuse reflectance spectra for the bulk powders.

Cold tests with a new diffuse reflectance probe made by Hellma are promising (Figure 4-3). The reflectance spectrum collected with approximately 20 mg Tm_2O_3, the new probe, and Ocean Insight spectrophotometers looks fantastic. With integration times <100 ms, this new approach should be amenable to collecting data on PuO_2 samples directly in the glove box. It would also be interesting to compare the bulk measurements with the Hellma probe (~ 20 mg) to single particle measurements collected with the new CRAIC micro-spectrometer (Figure 4-5).

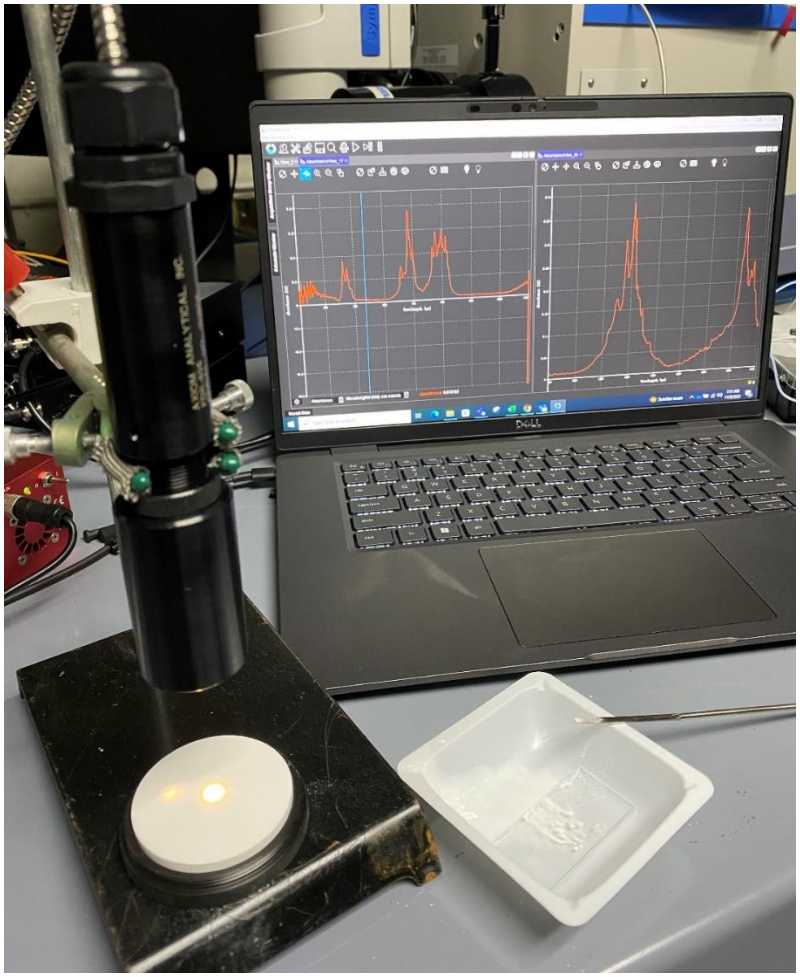

Figure 4-3. New diffuse reflection setup with a Gladius 805 probe (Hellma).

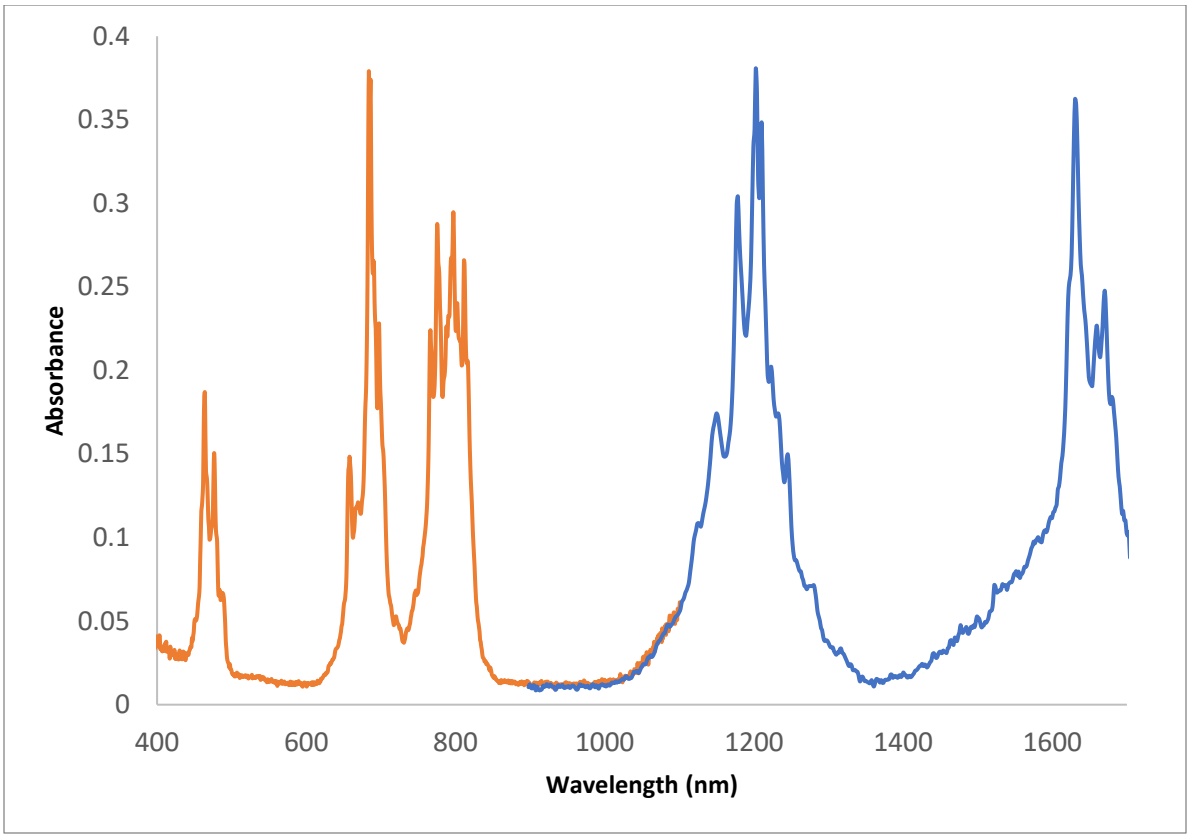

Figure 4-4. Tm_2O_3 diffuse reflectance spectrum collected with Hellma probe.

Figure 4-5. New CRAIC micro-spectrometer.

5. LASER-INDUCED BREAKDOWN SPECTROSCOPY

5.1 MOTIVATION

LIBS is a form of atomic emission spectroscopy that uses highly energetic laser pulses (i.e., the excitation source) to ablate samples and form a plasma. Each element emits light at characteristic frequencies when excited at plasma temperatures. Spectral features can be used to determine the relative abundance or concentration of impurities qualitatively or quantitatively. For example, LIBS could be useful for detecting trace impurities such as Fe, C, Si, or P relative to Pu.[28]

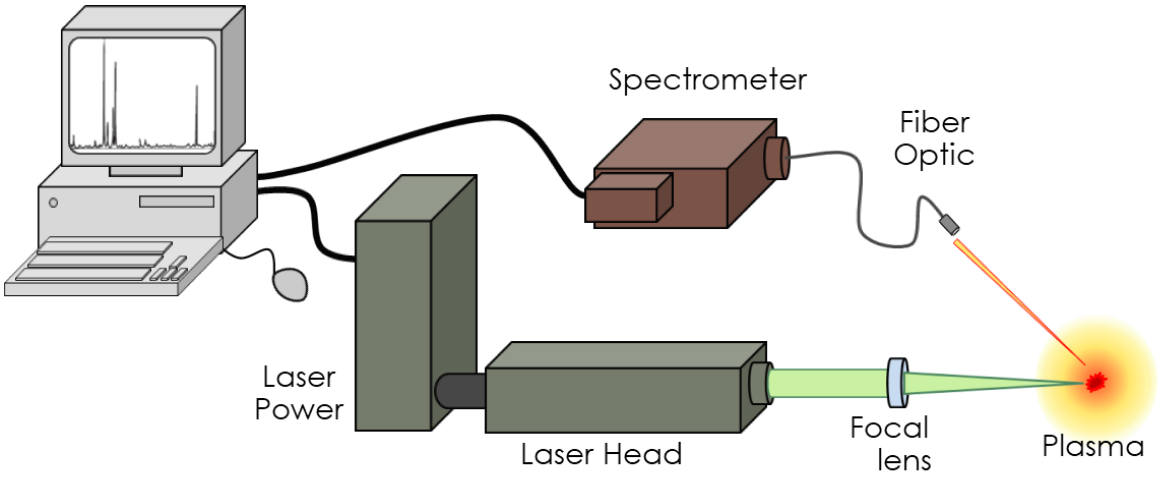

Figure 5-1. Notional LIBS schematic.

Elemental analysis with LIBS has several benefits including little to no sample preparation; analysis of solid, liquid, and gas phases; low detection limits in the parts per million range; quasinondestructive (nanograms per shot); and can be completely fiber optic–based. Some limitations include difficulty building calibration data sets because of matrix effects and limited spectral databases.

ORNL is establishing calibration-free methods to quantify actinide materials and trace impurities. Researchers can measure relatively large amounts of oxide material on a benchtop in sealed vessels. Proof-of-principle concepts were established in a recent publication documenting the first demonstration of calibration-free LIBS with a transuranium element. The methodology used to characterize Np samples can readily be extended to Pu.[29] Synergy is occurring between the scope outlined here and the capabilities being developed to support the ^{238}Pu Supply Program at ORNL.

5.2 RESULTS AND DISCUSSION

Previous LIBS work with Np used a 3D-printed chamber.[29] In this work, a more robust chamber using off-the-shelf parts was developed (Figure 5-2). The new LIBS compartment comprised off-the-shelf parts from Kurt J. Lesker and ThorLabs (Figure 5-2). The antireflective optical window will allow the incident laser and resulting signal to pass in and out while the chamber remains completely sealed. The Al blank flange, where the samples will be placed at the base, can readily be changed between each sample. Future work plans to prepare Pu samples in this sample chamber in a radiological hood, then the samples will be analyzed in a cold area with RCT support. A LIBS spectrum of the Al blank with relevant peaks are shown in Figure 5-3.

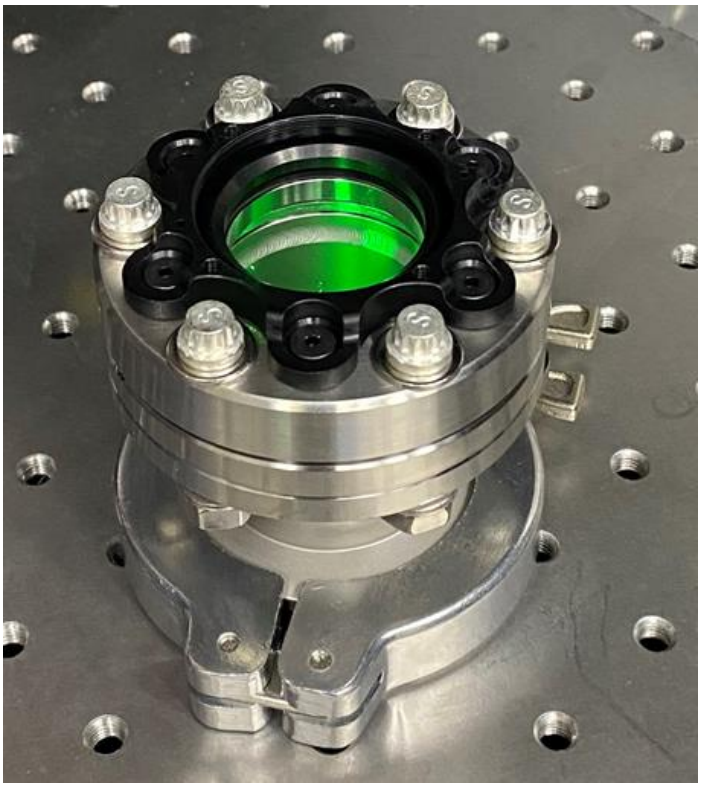

Figure 5-2. LIBS sample chamber.

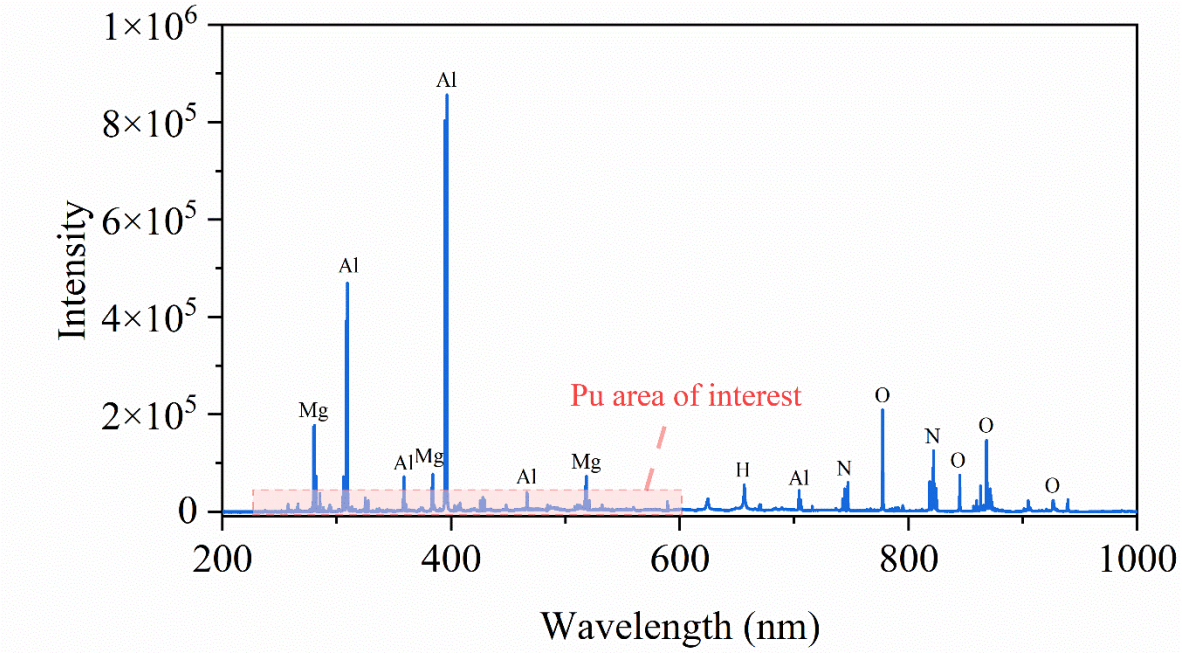

Figure 5-3. LIBS spectrum of Al blank with labeled peaks.

Several cold tests with CeO_2 were conducted prior to analyzing PuO_2 using a J200 (Applied Spectra). With respect to LIBS, CeO_2 is a reasonable surrogate for PuO_2 because the Ce(I) spectrum is composed of numerous peaks. For the initial demonstration, researchers analyzed CeO_2, Na_3PO_4, and Na_2SO_4 powders separately on C tape. Common impurities of interest to the science center and other ORNL programs,

such as the ^{238}Pu Supply Program, include S and P, which tend to have relatively weak emission peaks owing to the small energy gap compared with other impurities, such as transition metals (e.g., Fe) and short lifetimes. The spectrometer gating and laser pulse energy were adjusted to obtain an adequate signal.

Several line accumulations were averaged for each specimen. The shockwave from the laser clearly disrupted the particles (Figure 5-4). However, the samples did ablate, and representative spectra were obtained (Figure 5-5 and Figure 5-6).

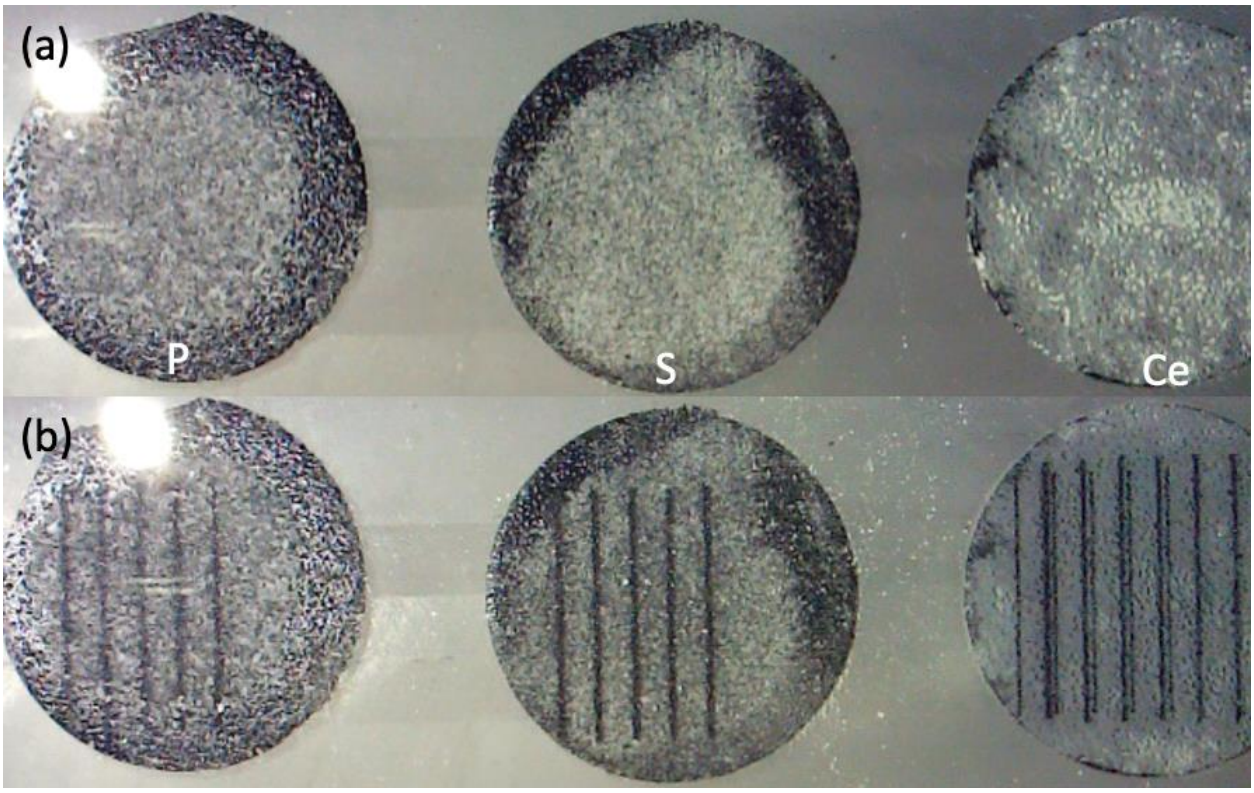

Figure 5-4. Powders prepared on C tape (a) before analysis and (b) after ablation.

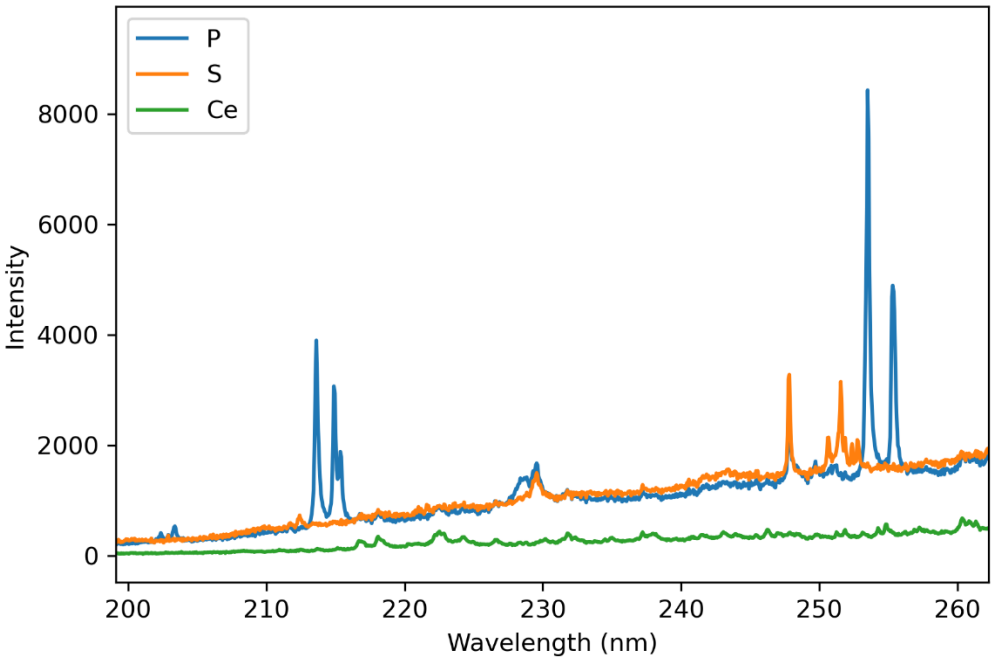

Figure 5-5. P peaks identified in the ultraviolet region.

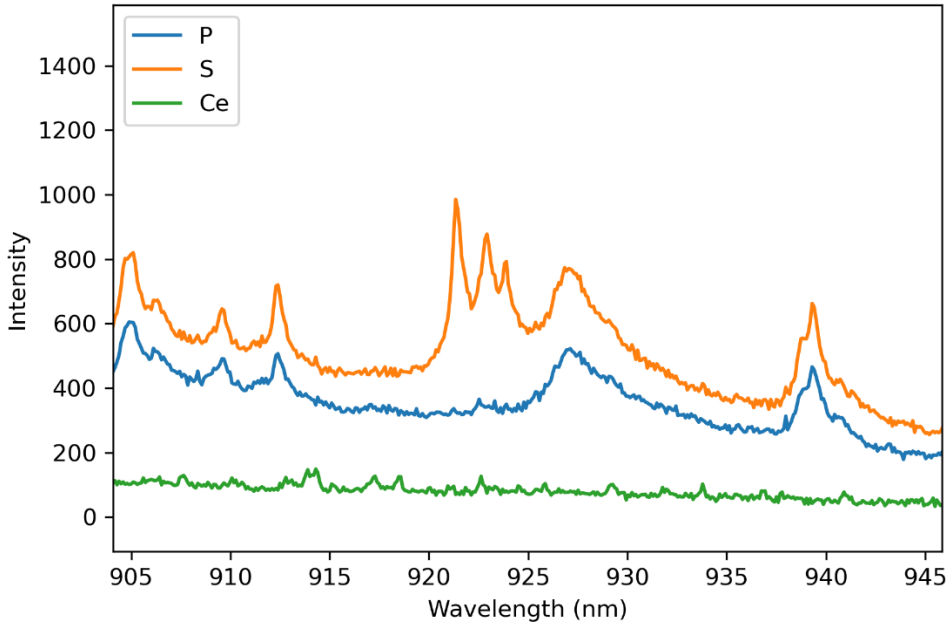

Figure 5-6. S peaks identified in the near infrared region.

5.3 NEXT STEPS

The authors plan to perform a systematic study in FY 2023 using surrogates to optimize the sample geometry and data acquisition parameters. Then, researchers will begin analyzing PuO_2 samples. If the sample is analyzed in an inert atmosphere, it would also be possible to determine an oxygen concentration

with enough precision to determine stoichiometry. It is also potentially possible to study morphology and particle size ablation efficiency correlation. This study would be a high-risk, high-reward possibility. Researchers with safety engineers and facility managers want to equip a glove box and hot cell environments with LIBS, but current regulations will not allow this. Work control development is ongoing.

6. FUTURE WORK AND CONCLUSIONS

6.1 FUTURE WORK

6.1.1 Laser fluorescence

ORNL has a Horiba Fluorolog-QM spectrometer for measuring luminescence steady-state emission and excitation spectra and lifetimes.[30] FY 2023 plans will include the analysis of slides containing PuO_2. The slides can be mounted at 22.5° using the solid sample holder. Researchers will attempt to measure luminescence spectra and lifetimes. Although PuO_2 is not fluorescent, fluorescence signatures have been noted as the sample degrades, potentially because of structural defects. Lifetimes may be collected with a Fluorolog-QM spectrometer (Horiba) and a DeltaTime kit for a DeltaDiode 405 nm laser (DD-405L) source operating with an average power of 2 mW and an average pulse width of 50 ps. A continuous wave LBX 405 nm laser (Oxxius) operating at 100 mW will be used to measure steady-state spectra. A broadband Xe arc lamp can be used to measure emission spectra as a function of different excitation energies.

6.1.2 SEM/energy dispersive spectroscopy

The ORNL Isotope Program purchased a benchtop SEM/energy dispersive spectroscopy unit that will be installed in a new glove box in the spring of FY 2023. This instrument will be shared between numerous projects at ORNL. When this instrument is installed and operating, researchers intend to characterize PuO_2 samples by SEM/energy dispersive spectroscopy to add another technique to ORNL's collection.

6.1.3 Neutron diffraction

Neutron diffraction and inelastic scattering can be used to characterize PuO_2.[31,32] The most logical facility to use would be the High Flux Isotope Reactor. Providing theoretical physicists with experimental data on PuO_2 would be a major feat. This technique is another high-risk, high-reward endeavor. Novel signatures may be discovered because this technique has not been studied in detail. Obtaining beam time may be difficult for a proposal that is purely exploratory (temperature and pressure effects). ORNL could perform density functional theory calculations beforehand or look in the literature to see if calculations have been done prior to submitting a proposal. The authors recently established the ability to study transuranium elements (i.e., NpO_2) using the High Flux Isotope Reactor's neutron powder diffraction facility.[33]

Neutron diffraction data will be collected as a function of the following parameters:

1. Temperature—learn about lattice expansion
2. Pressure—this is a significant unknown, possibly phase transition, new crystal structure, or an insulator
3. Magnetic field—provide information about magnetic properties
4. Diffraction data on sub- and superstoichiometric PuO_x—this may be the direction necessary. The data will be coupled with Raman spectroscopy to give the full picture of what is happening on the atomic level.

6.1.4 Reference materials and instrument transfer functions

ORNL is also interested in pursuing the developing of reference materials or instrument transfer functions for techniques like Raman spectroscopy.[34,35] This would assist the program by defining how to compare, validate, and optimize data acquisition parameters and interpretations between laboratories. Certain capabilities could be developed using surrogate materials (e.g., CeO_2) to reduce costs. The developed technology and methods could then be applied to Pu. This would allow future experiments to focus more directly on discovering and validating unique signatures in PuO_2.

6.2 CONCLUSIONS

This work established pertinent pathways for analyzing PuO_2 samples at ORNL. The study provided pXRD, Raman spectroscopy, and preliminary diffuse reflectance data. PCA was used to describe Raman spectral data sets. Future work may include a more detailed Raman or PCA study to help understand whether single samples represent the bulk process and how to capture statistically significant data with minimal analytical effort. These questions may be addressed using experimental design. This work also discussed paths forward for additionally improving techniques such as DRS and including new capabilities such as LIBS to further characterize future samples.

7. REFERENCES

[1] M. H. Rand, A. C. Fox, and R. S. Street, "Radiation Self-Damage in Plutonium Compounds," *Nature* 195 (1962): 567–568.

[2] J. H. Christian, B. J. Foley, E. Ciprian, D. D. Dick, M. Said, J. Darvin, A. E. Hixon, and E. Villa-Aleman, "Raman and infrared spectra of plutonium (IV) oxalate and its thermal degradation products," *J. Nucl. Mater.* 562 (2022): 153574.

[3] E. Villa-Aleman, J. H. Christian, J. R. Darvin, B. J. Foley, D. D. Dick, B. Fallin, and K. A. S. Fessler, "Diffuse Reflectance Spectroscopy and Principal Component Analysis to Retrospectively Determine Production History of Plutonium Dioxide," *Appl. Spectrosc.* (2022), DOI: 10.1177/00037028221145724.

[4] L. R. Sadergaski, K. G. Myhre, and L. H. Delmau, "Multivariate Chemometric Methods and Vis-NIR Spectrophotometry for Monitoring Plutonium-238 Anion Exchange Column Effluent in a Radiochemical Hot Cell," *Talanta Open* 5 (2022): 100120.

[5] M. Noe and J. Fuger, "Self-radiation effects on the lattice parameter of $^{238}PuO_2$," *Inorg. Nucl. Chem. Lett.* 10, (1974): 7–19.

[6] M. Naji, N. Magnani, L. J. Bonales, S. Mastromarino, J.-Y. Colle, J. Cobos, and D. Manara, "Raman spectrum of plutonium dioxide: Vibrational and crystal field modes." *Phys. Rev. B* 95 (2017): 104307.

[7] D. Manara, M. Naji, S. Mastromarino, J. M. Elorrieta, N. Magnani, L. Martel, and J.-Y. Colle, "The Raman fingerprint of plutonium dioxide: Some example applications for the detection of PuO_2 in host matrices," *J. Nucl. Mater.* 499 (2018): 268–271.

[8] E. Villa-Aleman, A. L. Houk, N. J. Bridges, and T. C. Shehee, "Raman spectroscopy: A tool to investigate alpha decay damage in a PuO_2 crystal lattice and determining sample age since calcination," *J. Raman Spectrosc.* 50, (2019): 899–901.

[9] E. Villa-Aleman, N. J. Bridges, T. C. Shehee, and A. L. Houk, "Raman microspectroscopy of PuO_2 particulate aggregates," *J. Nucl. Mater.* 515 (2019): 140–149.

[10] D. E. Hobart, "Diffuse Reflectance Spectroscopy of Plutonium Solids," *Actinide Res. Q.* 2 (2011): 37–41.

[11] J. L. Drummond and G. A. Welch, "The Preparation and Properties of Some Plutonium Compounds. Part VI. Plutonium Dioxide," *J. Chem. Soc.* (1957): 4781–4785.

[12] J. A. Porter and A. E. Symonds, Jr., *Precipitation of Plutonium(III) Oxalate and Calcination to Plutonium Oxide,* DP-981 (Aiken, South Carolina: E. I. Du Pont de Nemours & Co., Savannah River Laboratory, 1965).

[13] R. H. Condit, *Plutonium: An Introduction,* UCRL-JC-115357 (Livermore, California: Lawrence Livermore National Laboratory, 1993).

[14] L. V. Jones, D. Ofte, K. D. Phipps, and P. A. Tucker, "Preparation and Properties of Plutonium-bearing Oxide Particulates," *I&EC Prod. R&D* 3 (1964): 78–82.

[15] C. E. Holley, Jr., R. N. R. Mulford, E. J. Huber, Jr., E. L. Head, F. H. Ellinger, and C. W. Bjorklund, *Thermodynamics and Phase Relationships for Plutonium Oxides,* A/Conf.15/P/701 (Los Alamos Scientific Laboratory, Second United Nations International Conference on the Peaceful Uses of Atomic Energy, June 1958).

[16] D. A. Hoover, *Packaging and Transportation of Plutonium from Fuel Processing Plants,* ARH-SA-172 (Richland, Washington: Atlantic Richfield Hanford Company, 1973).

[17] J. C. Hindman, "Neptunium and Plutonium," *J. Chem. Educ.* 36 (1959): 22–26.

[18] D. Nickerson, "History of the Munsell Color System and Its Scientific Application," *J. Optical Soc. Am.* 30, no. 12 (1940): 575–586.

[19] R. Benz, R. M. Douglass, F. H. Kruse, and R. A. Penneman, "Preparation and Properties of Several Ammonium Uranium(IV) and Ammonium Plutonium(IV) Fluorides," *Inorg. Chem.* 2 (1963): 799–803.

[20] S. A. Pattenaude, N. H. Anderson, S. C. Bart, A. J. Gaunt, and B. L. Scott, "Non-aqueous Neptunium and Plutonium Redox Behaviour in THF—Access to a Rare Np(III) Synthetic Precursor," *Chem. Comm.* 48 (2018): 6077–6214.

[21] S. Wang, E. M. Villa, J. Diwu, E. V. Alekseev, W. Depmeier, and T. E. Albrecht-Schmitt, "Role of Anions and Reaction Conditions in the Preparation of Uranium(VI), Neptunium(VI), and Plutonium(VI) Borates," *Inorg. Chem.* 50 (2011): 2527–2533.

[22] S. K. Cary, S. S. Galley, M. L. Marsh, R. E. Baumbach, J. N. Cross, J. T. Stritzinger, M. J. Polinski, L. Maron, and T. E. Albrecht-Schmitt, "Incipient Class II Mixed-Valency in a Plutonium Material," *Nat. Chem.* 9 (2017): 856–861.

[23] M. Runowski, N. Stopikowska, and S. Lis, "UV-Vis-NIR absorption spectra of lanthanide oxides and fluorides," *Dalton Trans.* 49 (2020): 2129–2137.

[24] J. D. Einkauf and J. D. Burns, "Solid state characterization of oxidized actinides co-crystallized with uranyl nitrate hexahydrate," *Dalton Trans.* 49 (2020): 608–612.

[25] H. G. Hecht, "The Interpretation of Diffuse Reflectance Spectra," *J. Res. Nat. Bur. Stds.* 80A, (1976): 567–583.

[26] B. E. Bernacki, T. J. Johnson, and T. L Myers, "Modeling thin layers of analytes on substrates for spectral analysis: Use of solid/liquid *n* and *k* values to model reflectance spectra," *Opt. Eng.* 59, no. 9 (2020): 092005.

[27] T. M. McCleskey, E. Bauer, Q. Jia, A. K. Burrell, B. L. Scott, S. D. Conradson, A. Mueller, L. Roy, X. Wen, G. E. Scuseria, and R. L. Martin, "Optical band gap of NpO_2 and PuO_2 from optical absorbance of epitaxial films," *J. Appl. Phys.* 113 (2013): 013515.

[28] K. G. Myhre, H. B. Andrews, D. Sulejmanovic, C. I. Contescu, J. R. Keiser, and N. C. Gallego, "Approach to using 3D laser-induced breakdown spectroscopy (LIBS) data to explore the interaction of FLiNaK and FLiBe molten salts with nuclear grade graphite," *J. Anal. At. Spectrom.* 37 (2022): 1629–1641.

[29] H. B. Andrews, L. R. Sadergaski, and K. G. Myhre, "Neptunium transition probabilities estimated through laser induced breakdown spectroscopy (LIBS) measurements," *J. Anal. At. Spectrom.* 37 (2022): 768–774.

[30] L. R. Sadergaski and H. B. Andrews, "Simultaneous quantification of uranium(VI), samarium, nitric acid, and temperature with combined ensemble learning, laser fluorescence and Raman scattering for real-time monitoring," *Analyst* 147 (2022): 4014–4025.

[31] P. Zhang, B.-T. Wang, and X.-G. Zhao, "Ground-state properties and high-pressure behavior of plutonium dioxide: Density functional theory calculations," *Phys. Rev. B.* 82 (2010): 144110.

[32] M. Janoschek, P. Das, B. Chakrobarti, D. L. Abernathy, M. D. Lumsden, J. M. Lawrence, J. D. Thompson, G. H. Lander, J. N. Mitchell, S. Richmond, M. Ramos, F. Trouw, J.-X. Zhu, K. Haule, G. Kotliar, and E. D. Bauer, "The valence-fluctuating ground state of plutonium," *Sci. Adv.* 1, (2015): 1500188.

[33] M. D. Frontzek, L. R. Sadergaski, S. K. Cary, and B. K. Rai, "Search for octupolar order in NpO_2 by neutron powder diffraction," *J. Solid State Chem.* 321 (2023): 123875.

[34] A. Ntziouni, J. Thomson, I. Xiarchos, X. Li, M. A. Banares, C. Charitidis, R. Portela, E. L. Diz, Review of Existing Standards, Guides, and Practices for Raman Spectroscopy. *Appl. Spectrosc.* 76, (2022): 747-772.

[35] Y-L. Lin, Sinfield, J. V. Characterization of Raman Spectroscopy System Transfer Functions in Intensity, Wavelength, and Time. Instruments. 4, (2020): 4030022.